Thermodynamic Study on λ-Ti_3O_5 Exhibiting a Light-induced Metal-Semiconductor Transition

Hiroko Tokoro[a,b] and Shin-ichi Ohkoshi,[a,c,*]

[a] *Department of Chemistry, School of Science, The University of Tokyo, 7-3-1 Hongo, Bunkyo-ku, Tokyo 113-0033, Japan,* [b] *NEXT, JSPS, 8 Ichibancho, Chiyoda-ku, Tokyo 102-8472, Japan,* [c] *CREST, JST, 5 Sanbancho, Chiyoda-ku, Tokyo 102-0075, Japan*

I. Introduction

Titanium oxide including Ti_2O_3, Ti_3O_5 and Ti_4O_7, which is called black titanium oxide due to its color, exhibits a metal-semiconductor transition. For example, Ti_3O_5 exhibits the β-phase (semiconductor) below 460 K, but is in the α-phase (metallic conductor) above 460 K. To date, studies on black titanium oxide have been limited in bulk or single crystals; the physical properties of nanoparticles are not well studied. However, we recently synthesized a novel type black titanium oxide, λ-Ti_3O_5 nanoparticles, which exhibit a metallic electric conductivity and a light-induced metal-semiconductor transition to β-Ti_3O_5 at room temperature.[1] λ-Ti_3O_5 is the first observed example of a metal oxide with a room-temperature light-induced phase transition. Herein first principle calculation and statistical thermodynamics calculation are carried out to investigate the electronic states of the λ-Ti_3O_5 and to discuss the mechanism for the light-induced metal-semiconductor transition.

II. Crystal structure and fundamental physical properties of λ-Ti_3O_5

Either a chemical method combining the reverse micelle and sol-gel methods or calcinating TiO_2 nanoparticles in a hydrogen atmosphere yields λ-Ti_3O_5 with a *C*2/*m* monoclinic crystal structure (a = 9.8378(5) Å, b = 3.78674(11) Å, c = 9.9707(3) Å, and β = 91.257(3)°) (Fig 1). λ-Ti_3O_5 has an electric conductivity of $\sigma = 3\times10^{1}$ S cm^{-1}, and exhibits a metallic absorption band. The relationship between coupling length and atomic valence obtained from Rietveld analysis indicates the valence states of Ti(1), Ti(2), and Ti(3) in λ-Ti_3O_5 are 3.37, 3.20, and 3.53, respectively, which are close to the values for a charge-delocalized system, $(Ti^{3\frac{1}{3}+})_3$. On the other hand, semiconducting β-Ti_3O_5 is a *C*2/*m* monoclinic crystal (a = 9.748(1) Å, b = 3.8013(4) Å, c = 9.4405(7) Å, and β = 91.529(7)°) with an electric conductivity of $\sigma = 3\times10^{-2}$ S cm^{-1} and a band gap of 0.14 eV. The relationship between the coupling length and atomic valence indicates the valence states of β-Ti_3O_5 are 3.00, 3.79, and 3.32, which are close to the valence states of a charge-delocalized system, $(Ti^{3+}-Ti^{3\frac{2}{3}+}-Ti^{3\frac{1}{3}+})$.

III. First principle calculations of the electronic states of λ-Ti_3O_5

We performed first principle calculation of the band structure of Ti_3O_5 using the Vienna *ab initio* simulation package (VASP). Because the first principle calculation for Ti_3O_5 has not reported yet, we first performed a calculation on β-Ti_3O_5, which exhibits semiconducting properties. The energy levels of the Ti *3d*-orbital and O *2p*-orbital near the Fermi level in the density of states diagram indicate that β-Ti_3O_5 is a Mott-Hubbard type semiconductor (Fig. 2), and the nearest d_{xy}-orbitals of Ti(3) are σ–coupled to form a Ti(3)-Ti(3) bipolaron with a valence band at –0.60 eV. Additionally, a Ti(1)-Ti(1) bipolaron forms a band at the lower energy level of –1.35 eV.

On the other hand, the empty d_{xz}-orbital of Ti(2) mainly forms the conduction band near +0.71 eV (Fig. 3). The estimated energy difference between the valence and conduction bands, i.e., the band gap, is 0.13 eV, which is consistent with that from the reflectance spectrum (0.14 eV).

In contrast, the valence and conduction bands of β-Ti_3O_5 are hybridized in λ-Ti_3O_5, and the Ti(2) d_{xy}– and d_{xy}–orbitals are π–stacked to form a charge-delocalized band, which extends one-dimensionally in the *b*-axis direction of the crystal, leading to the missing of the band gap. This hybridization is thought to be the origin of the metallic electric conductivity in λ-Ti_3O_5. It should be noted that the band due to the Ti(1)-Ti(1) bipolaron is located at –0.58 eV.

IV. Thermodynamic analysis of the light-induced phase transition mechanism

Thermodynamic analysis was performed to understand the mechanism of the light-induced reversible phase transition on λ-Ti_3O_5 using the Slichter-Drickamer (SD) model, a mean field approximation. First, the relationship between the Gibbs free energy (G) and the transition fraction for the first-order phase transition on bulk sample from β-Ti_3O_5 to α-Ti_3O_5 phases was indicated. Here, a

charge-localized unit ($Ti^{3+}-Ti^{3\frac{2}{3}+}-Ti^{3\frac{1}{3}+}$)$O_5$ and charge-delocalized unit ($Ti^{3\frac{1}{3}+}$)$_3O_5$ were used as the order parameters to indicate the transition fraction (Fig. 4). The increase of charge-delocalized unit expresses the increase of the transition fraction. Differential scanning calorimetry (DSC) of β-Ti_3O_5 produced one peak as the temperature increased. The peak corresponds to a first-order phase transition, and gives ΔH = 13.3 kJ mol^{-1} and ΔS = 29.4 J K^{-1} mol^{-1}. The SD model calculation using these obtained thermodynamic parameters and an interaction parameter (γ) of 9.3 kJ mol^{-1} reproduces the metal-semiconductor transition between β-Ti_3O_5 and α-Ti_3O_5 phases on bulk sample (Fig. 5, right). In contrast, DSC does not exhibit a peak in the transition between λ-Ti_3O_5 and α-Ti_3O_5 phases (Fig. 5, left), indicating the transition from the λ-phase to the α-phase is a second order phase transition. Using a pressure effect from λ-Ti_3O_5 to β-Ti_3O_5, we experimentally obtained the thermodynamic parameters for the phase transition of Ti_3O_5 nanoparticles. The results gives ΔH = 4.8 kJ mol^{-1} and ΔS = 10.4 J K^{-1} mol^{-1}, which are approximately 40% of those of bulk sample.

Next, we performed SD calculations using obtained ΔH and ΔS values and assuming that γ is similar to that of bulk sample (9.0 kJ mol^{-1}). An energy barrier between the charge-localized system and charge-delocalized system occurs over the entire temperature range in the Gibbs free energy (Fig. 5, left), and the charge-delocalized system is maintained as the temperature is decreased from the calcination temperature of 1200 °C. The calculations represent that λ-Ti_3O_5 is a metallic conductor with a charge-delocalized system, and that the phase transition between λ-Ti_3O_5 and α-Ti_3O_5 is a second-order phase transition. Additionally, the calculation results indicates that the β-Ti_3O_5 is the hidden true stable phase below 460 K. Hence, from a thermodynamic viewpoint, the observed light-induced metal-semiconductor transition is a phase transition from λ-Ti_3O_5 trapped in an energy-minimum state to the hidden stable phase of β-Ti_3O_5. Furthermore, the metallic absorption of λ-Ti_3O_5 indicates that the light-induced metal-semiconductor transition can be induced by using nanosecond pulse laser irradiation of 355, 532, or 1064 nm. In contrast, the light-induced phase transition in the reverse direction from β-Ti_3O_5 to λ-Ti_3O_5 is thought to be a transition to λ-Ti_3O_5 via excitation from the valence band to the conduction band of β-Ti_3O_5, caused by pulsed laser irradiation. The photo-thermal effect from continuous semiconductor laser irradiation may cause a transition from β-Ti_3O_5 to λ-Ti_3O_5 via α-Ti_3O_5 (β-Ti_3O_5 → α-Ti_3O_5 → λ-Ti_3O_5)

V. Summary

First principle and statistical thermodynamic calculations were performed on the light-induced phase transition of a novel titanium oxide λ-Ti_3O_5 through a nanosize effect. First principle calculations indicated that λ-Ti_3O_5 and β-Ti_3O_5 possess a metallic conductor-type band structure and a semiconductor-type band structure, respectively, while statistical thermodynamic calculations indicated that a breakdown of the light-induced phase between the metastable phase, which is a thermodynamically trapped local minimum, and a true stable phase can explain this phase transition. Light-induced phase change materials, e.g., chalcogen compounds, have been practically used as optical data strage.[2,3] λ-Ti_3O_5 could be a new candidate for optical storage material for the next generation, since λ-Ti_3O_5 possess the advantage that Ti is environmentally benign element.

Acknowledgements

This work was performed under the management of the Project to Create Photocatalyst Industry for Recycling-oriented Society supported by NEDO. We are thankful for the CREST project of JST, Grant-in-Aid for Young Scientists (S) from JSPS, NEXT program from JSPS, and Asahi Glass Foundation. We acknowledge the Cryogenic Research Center, The University of Tokyo, and the Center for Nano Lithography & Analysis, The University of Tokyo, supported by MEXT Japan.

References

1. S. Ohkoshi, Y. Tsunobuchi, T. Matsuda, K. Hashimoto, A. Namai, F. Hakoe, H. Tokoro, ***Nature Chem.***, 2, 539 (2010).
   [This paper is highlighted in ***Nature Chemistry***, "News & Views", 2, 517 (2010); ***Nature Materials***, "Commentary", 10, 158 (2011); ***Nature Japan***, "Special reports", 2010.6.25]
2. N. Yamada, E. Ohno, K. Nishiuchi, N. Akahira, M. Takao, ***J. Appl. Phys.***, 69, 2849 (1991).
3. M. Wuttig, and N. Yamada, ***Nature Mater.***, 6, 824 (2007).

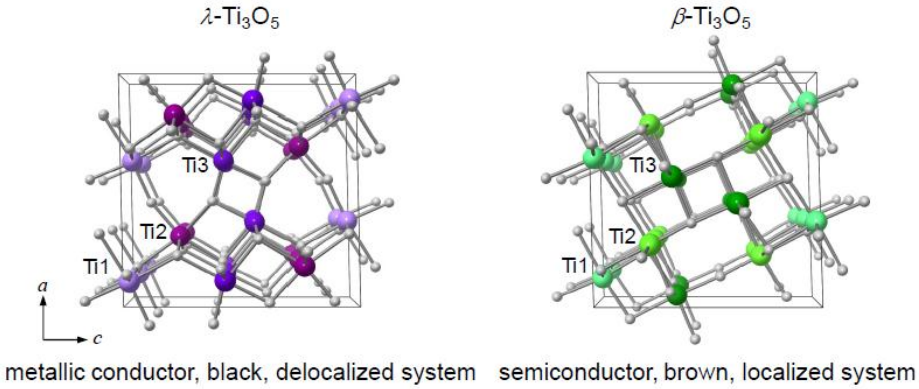

Fig. 1, Crystal structures of λ-Ti_3O_5 (left) and β-Ti_3O_5 (right).

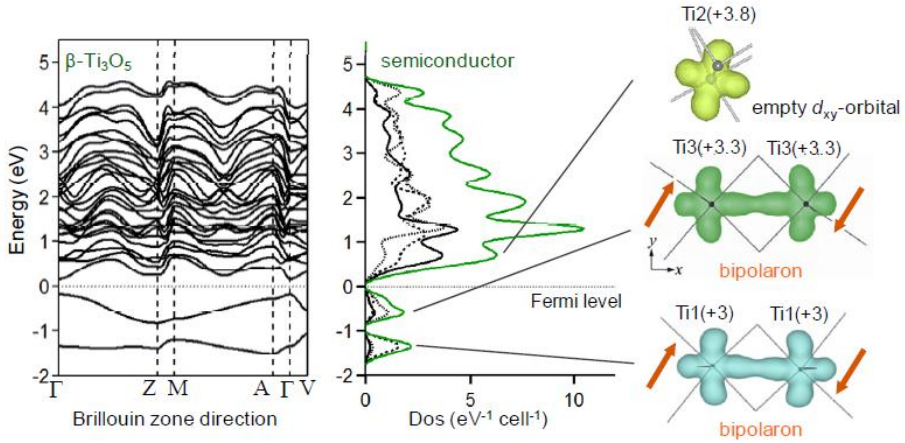

Fig. 2, First principle calculation for β-Ti_3O_5. Band diagram (left), density of states diagram with Ti1 (---), Ti2 (—), Ti3 (···), and total (▬) (middle), and schematic illustration of electron density diagram for Ti (right).

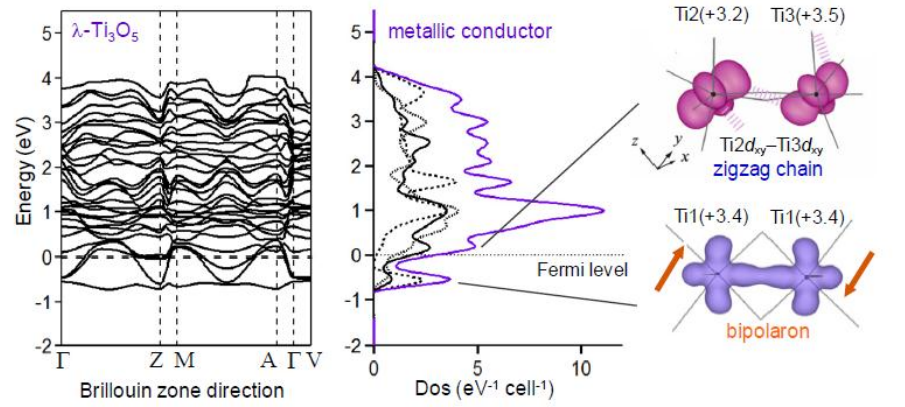

Fig. 3, First principle calculation for λ-Ti_3O_5. Band diagram (left), density of states diagram with Ti1 (---), Ti2 (—), Ti3 (···), and total (▬) (middle), and schematic illustration of electron density diagram for Ti (right).

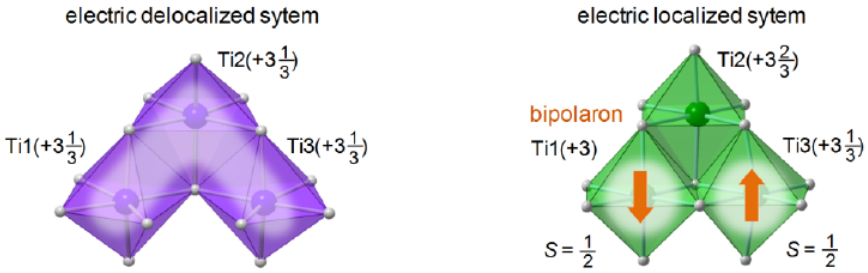

Fig. 4, Schematic diagram of a charge-delocalized unit (left) and charge-localized unit (right).

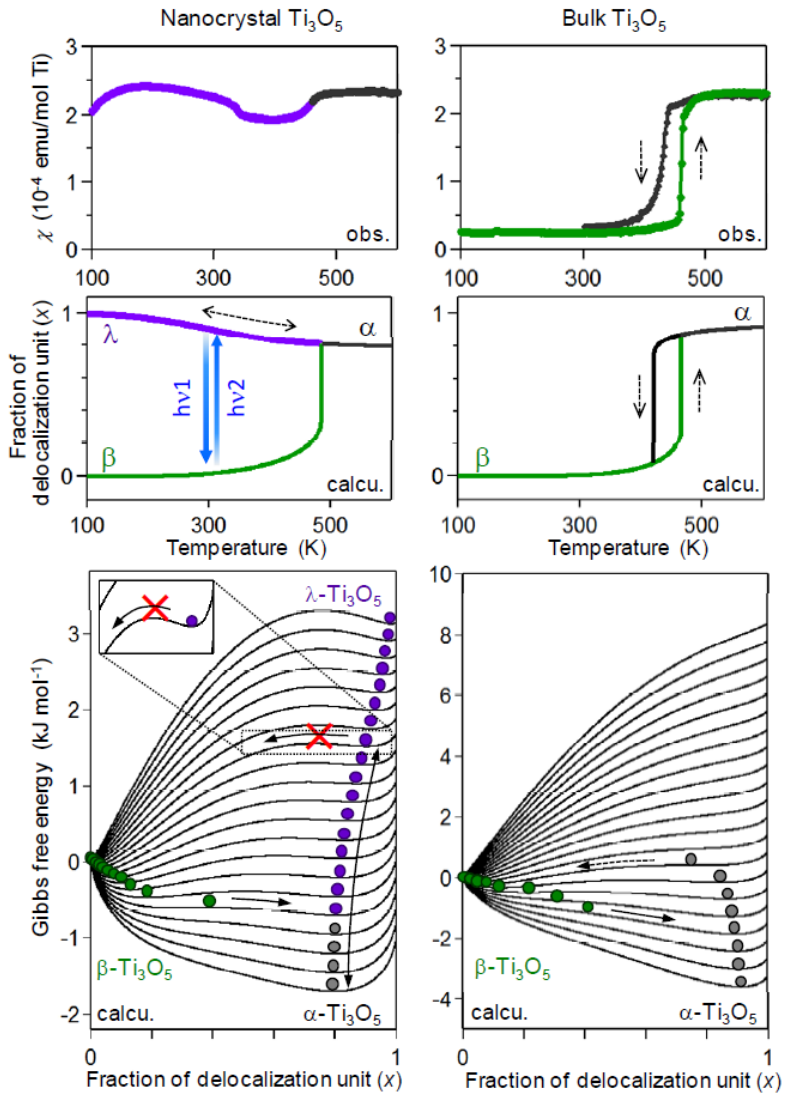

Fig. 5, Thermodynamic calculations on the phase transition in nanocrystal (left) and bulk (right) Ti_3O_5.